

Directed Growth of Fungal Hyphae in an Electric Field

A Biophysical Analysis

Hans Gruler

Department of Biophysics, University of Ulm, D-7900 Ulm, Bundesrepublik Deutschland
and

Neil A. R. Gow

Department of Genetics and Microbiology, Marischal College, University of Aberdeen,
Aberdeen AB9 1 AS, U.K.

Z. Naturforsch. **45c**, 306–313 (1990); received October 20, 1989/January 10, 1990

Galvanotropism, Dose-Response Curve, Mycelial Growth

The galvanotropic response of the mycelial fungus *Neurospora crassa* is investigated. The angle distribution function of growing hyphae is described by a generating function which contains two non-trivial terms; one for directional growth and one for bidirectional growth. The following results were obtained. (i) Germ tubes grew towards the anode. (ii) The cellular response was linear for small sized cells and weaker electric fields. The galvanotropic constant, K_{GROW} , which describes the linear response, was small for short germ tubes or hyphae ($K_{\text{GROW}}^{-1} = -20 \text{ V} \cdot \text{cm}^{-1}$ for $l_0 = 10 \text{ } \mu\text{m}$) and large for longer cells ($K_{\text{GROW}}^{-1} = -1.7 \text{ V} \cdot \text{cm}^{-1}$ for $l_0 = 100 \text{ } \mu\text{m}$). The growth coefficient K_p of (-18.5 mV) describes the response independent of cell size. The linear response is explained by the field-induced distribution of charged membrane-bound proteins essential for galvanotropism. (iii) For $E > E_0 = 3.8 \text{ V} \cdot \text{cm}^{-1}$, the linear response is inhibited (inhibition coefficient $K_1 = 1.11$). The inhibition is explained by field-induced changes of the membrane potential. (iv) The galvanotropic response of longer hyphae was bidirectional. The cells grew on average perpendicular to the applied field. The bidirectional response is proportional to E^2 with a bidirectional growth coefficient K_2 of $-(0.25 \text{ V})^{-2}$. The bidirectional growth is explained by the inhibition of the directed growth process. The transition from anode-directed to bidirectional growth was a function of the applied electric field as well as of the tube length (directed growth for $E^2 \cdot l_0 < 4.4 \text{ V}^2 \cdot \text{cm}^{-1}$ and bidirectional growth for $E^2 \cdot l_0 > 4.4 \text{ V}^2 \cdot \text{cm}^{-1}$).

Introduction

A variety of cells including leukocytes, macrophages, fibroblasts, amoebae, slime molds, etc. have the ability to direct their movement in an electric field. Some cell types like granulocytes, monocytes, etc. migrate towards the anode and other cell types like fibroblasts, neural crest cells, growth cones of neurones, grow towards the cathode [1]. The phenomenological description of these directed movements are quite well developed, however, the mechanisms behind the responses remain obscure.

The orientation or the average drift movement towards the anode or cathode can be predicted if (i) the magnitude of the applied electric field strength and (ii) intrinsic cellular properties quantified by the galvanotactic or galvanotropic coefficients, are known [2, 3]. In this paper we will show

that these phenomenological descriptions, already successfully applied to galvanotaxis [2, 3], chemotaxis [2, 3] and contact guidance [4] can also be applied to galvanotropism.

Galvanotropism is the ability of cells to direct their growth in an applied electric field. As in positive and negative galvanotaxis some cell types grow towards the cathode others to the anode [5]. For example, developing neurones [6], rhizoids of zygotes of *Fucus serratus* [7], hyphae and branches of *Aspergillus nidulans* [5], and of *Mucor mucedo* [5] grow towards the cathode. But rhizoids of zygotes of *Ulva* and *Fucus inflatus* [8–10], and the hyphae and branches of *Neurospora crassa*, and of *Achlya bisexualis* [5] grow towards the anode. Hyphal tips and germ tubes of *Phycomyces blakesleeenanus* grow towards the cathode at high electric field strengths ($E > 5 \text{ V} \cdot \text{cm}^{-1}$) and towards the anode at low field strengths [11]. A similar observation was made by McGillivray and Gow [5] for the mycelial growth of *Trichoderma harzianum*. The hyphae grew towards the cathode but the

Reprint requests to Prof. H. Gruler.

Verlag der Zeitschrift für Naturforschung, D-7400 Tübingen
0341–0382/90/0300–0306 \$ 01.30/0



Dieses Werk wurde im Jahr 2013 vom Verlag Zeitschrift für Naturforschung in Zusammenarbeit mit der Max-Planck-Gesellschaft zur Förderung der Wissenschaften e.V. digitalisiert und unter folgender Lizenz veröffentlicht: Creative Commons Namensnennung-Keine Bearbeitung 3.0 Deutschland Lizenz.

Zum 01.01.2015 ist eine Anpassung der Lizenzbedingungen (Entfall der Creative Commons Lizenzbedingung „Keine Bearbeitung“) beabsichtigt, um eine Nachnutzung auch im Rahmen zukünftiger wissenschaftlicher Nutzungsformen zu ermöglichen.

This work has been digitalized and published in 2013 by Verlag Zeitschrift für Naturforschung in cooperation with the Max Planck Society for the Advancement of Science under a Creative Commons Attribution-NoDerivs 3.0 Germany License.

On 01.01.2015 it is planned to change the License Conditions (the removal of the Creative Commons License condition "no derivative works"). This is to allow reuse in the area of future scientific usage.

branches were formed towards the anode. A simple model is presented which can explain these different cellular responses.

Before a molecular model for galvanotaxis and galvanotropism can be formulated it is necessary to have an accurate description of the directed growth and directed movement of the cells under investigation. Our mathematical analysis of directed movement and of directed growth is based on experimentally determined angle distribution functions. The method will be demonstrated for the galvanotropism of growing mycelial fungi where the angle distribution functions are already published [5]. This kind of mathematical analysis, however, is neither restricted to these types of cells nor to the analysis of electric fields. Other cell types growing in ordering fields such as magnetic fields, illumination by light, the concentration gradients of ions and of molecules, can be analyzed in an analogous way.

Materials and Methods

In order to perform this analysis a detailed knowledge of how the data were obtained from the experiments and then stored in form of a distribution function is necessary. In this context it is also preferable to have the whole distribution function for all cells in a population since a large amount of information is lost if the response of all the individual cells is averaged.

McGillivray and Gow [5] investigated the growth of hyphae *Neurospora crassa* RL 21a under the influence of an electric field. Conidia and agarose were mixed and poured onto a gel plate and electric fields were applied using a small DNA electrophoresis cell. (The low conducting media ($<5 \text{ mS} \cdot \text{cm}^{-1}$) contained 2% (w/v) malt extract and 20 mM-potassium phosphate buffer, pH 6.5). At the end of an experiment the gel was removed and fixed in formalin before examination.

Data Collection

The fixed specimens were observed within the gels using a microscope at low magnification (100X). The angle, Θ , of a germ tube or of a mature hypha with respect to the applied electric field was determined as long as the whole germ tube or a significant portion of the hyphae was in the focal plane. The frequency of the angles were represent-

ed in histograms $N(\Theta)$ for every growth process as shown in [5].

Before these histograms $N(\Theta)$ are analyzed in detail we have to know the accuracy of the measured angle Θ . It is not the statistical error of Θ which is of most concern but rather the systematic error in Θ . The problem is that the angle in a projection plane (focal plane) is determined in two dimensions, however we need the angle between the germ tube or hypha and the electric field in three dimensional space. A relationship between the actual angle Φ in the three dimensional space and the angle Θ determined in the projection plane can be determined in the following way. First let us assume that a germ tube of length l is within the projection plane so that the angle is determined by l and by the radical distance, r , of the hyphal tip to an electric field line, which extends to the conidium at the neck of the germ tube (see Fig. 1a). If the projection plane is rotated around the electric field vector where the conidium/germ tube junction is a fixed point then the lengths l' and r' and the angle Θ as seen in the new projection plane (see Fig. 1b) are altered. The angle Φ of the three-dimensional space can be expressed from the projected germ tube if r' , l' and Δx are measured (a similar approach can be used for hyphae).

$$\sin^2 \Phi = \frac{r'^2 + \Delta x^2}{l'^2 + \Delta x^2}. \quad (1)$$

How far the germ tubes deviate from the projection plane is described by Δx . This equation can be approximated for $\Delta x < l'$ to

$$\sin^2 \Phi = \sin^2 \Theta + \left(\frac{\Delta x}{l'}\right)^2 + \dots \text{(higher order terms)}. \quad (2)$$

$\Delta x/l'$ can be estimated from the depth of focus and the tube length, to be smaller than 0.1. This means

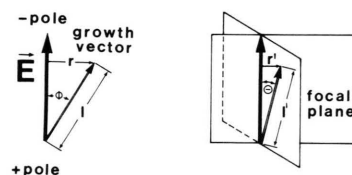


Fig. 1. Schematic representation of a germ tube in the viewing field. a) The germ tube is within an optical plane as seen in the light microscope. b) This coordinate system is rotated so that the germ tube makes an angle to the plane.

the angle determined from the projection plane (Θ) can be regarded as the real angle (Φ) between the oriented germ tube or hypha and the direction of the electric field.

Symmetry of the assay

The normalized histogram of the angle distribution function $f(\Phi)$ is the number of cells, $N(\Phi)$, in every segment of the histogram divided by the total number of cells $\Sigma N(\Phi)$. The experimental results have the following symmetry since the physical state described by Φ cannot be distinguished from the state described by $-\Phi$.

$$f(\Phi) = f(-\Phi). \quad (3)$$

Therefore it is not necessary to consider the whole distribution between -180° and $+180^\circ$. It is sufficient to consider $f(\Phi)$ between 0 and $+180^\circ$. The advantage of this procedure is that the number of cells in every segment in the histogram can be increased by reassigning all negative angles to positive ones. Therefore the statistical error decreases since each segment now contains twice the number of measurements.

Every assay is checked for systematic errors by quantifying the deviation from the symmetry relation mentioned above. For example if the electric field vector is altered in its original direction then the mean of $\sin \Phi$ is no longer equal to zero. $\langle \sin \Phi \rangle$ is zero if the distribution is symmetrical (Eqn. [3]). The control parameter $|\langle \sin \Phi \rangle|$ was in all experiments less than 0.05.

Generating function

The angle distribution function, $f(\Phi)$, is always positive, and therefore it can be expressed by a new function, $V(\Phi)$, – the generating function – without losing information [12].

$$f(\Phi) = e^{V(\Phi)}. \quad (4)$$

In the next step, $V(\Phi)$ is described by a Fourier series [2, 3].

In physical systems the generating function has a theoretical background: the Boltzmann factor which is the integrated force or torque divided by the thermal energy. In biological systems the generating function is equivalent to the integrated primary cellular signal divided by the square of the

noise amplitude in the signal transduction system [13].

One obtains after applying the symmetry operation (Eqn. (3)).

$$V(\Phi; E) = a_0(E) + a_1(E) \cdot \cos \Phi + a_2(E) \cdot \cos 2 \Phi + \dots \quad (5)$$

The unknown coefficients $a_0(E)$, $a_1(E)$, \dots , are determined by fitting Eqn. (4) and (5) to the experimentally determined distribution function. For this fit the natural logarithm of the experimentally determined angle distribution function is plotted versus $\cos \Phi$.

The calculation of $\ln f(\Phi)$ often presents some problems when the number of data points is low since then it is not uncommon to find several segments of the histogram unoccupied. $\ln f(\Phi)$ would be undefined ($-\infty$) for such segments. One simple procedure is to replace the value of each segment with the average of that segment and its two closest neighbours. Then, only if all three segments have an “ N ” of zero will the average be zero. In most cases this will provide a non-zero value, and will also smooth out the distribution. If there are still sharp discontinuities in the distribution, this procedure can be repeated a second time. For highly oriented distributions, it is not uncommon to find large regions with $N(\Phi) = 0$. In these instances the distribution can only be evaluated over the non-zero region. After data smoothing is performed, the natural logarithm of each segment, $\ln f(\Phi)$, is calculated and plotted versus $\cos \Phi$ to determine $a_0(E)$, $a_1(E)$, $a_2(E)$, \dots . These coefficients can be interpreted as follows:

(i) The coefficient $a_0(E)$ is the least important term describing only the calibration of the distribution function.

(ii) The coefficient $a_1(E)$ describes the mean directed growth. For example $a_1 > 0$ and $a_2 = 0$, $a_3 = 0$, \dots , represent cells growing on average parallel to and in the direction of the electric field vector and $a_1 < 0$ and $a_2 = 0$, \dots , represent cells growing on average parallel to but opposite to the electric field vector. The plot of $\ln f(\Phi)$ vs. $\cos \Phi$ is a straight line in this case. The slope of the line yields the coefficient a_1 . When $|a_1|$ is large the angle distribution is narrow; when $|a_1|$ is small the distribution is broad.

(iii) The coefficient $a_2(E)$ describes the mean bi-directional growth. For example $a_2 > 0$ and $a_1 = 0$,

$a_3 = 0, \dots$, the cells grow on average with the same probability parallel and antiparallel to the electric field vector and for $a_2 < 0$ and $a_1 = 0, a_3 = 0, \dots$, the cells grow on average perpendicularly to the electric field. The plot of $\ln f(\Phi)$ vs. $\cos \Phi$ is a parabola in these cases. The curvature or more accurately the second derivative of this curve yields the coefficient a_2 . The angle distribution is narrow when $|a_2|$ is large and broad when $|a_2|$ is small.

Dose-response curve

The directed growth process can be quantified by the average of $\cos \Phi$ ($= \langle \cos \Phi \rangle = \langle P_1 \rangle$) [5].

$$\langle \cos \Phi \rangle = \int_0^{2\pi} \cos \Phi \cdot f(\Phi) \cdot d\Phi. \quad (6)$$

Eqn. (6) quantifies the average directed growth process in a plane (equivalent to the focal plane of the microscope). $\langle \cos \Phi \rangle$ is +1, when all cells grow parallel to E and towards the cathode. $\langle \cos \Phi \rangle$ is -1 when all the cells grow opposite to E towards the anode. $\langle \cos \Phi \rangle$ is zero when the cells grow with random orientation. McGillivray and Gow [5] multiplied $\langle \cos(\Phi - 180^\circ) \rangle$ by 100 and calling this "percentage polarization". The angle was defined with respect to the positive pole (anode). Φ is the angle between the growth vector and the electric field vector. Another frequently used definition measures the angle towards the cathode. The magnitude of $\langle \cos \Phi \rangle$ is the same irrespective of whether angles are measured with respect to the positive or the negative poles.

Eqn. (6) can be equated with Eqn. (4) by assuming that the angle distribution function has only one non-trivial term $a_1 \neq 0$ and $a_2 = 0, a_3 = 0, \dots$ (2, 3)

$$\langle \cos \Phi \rangle = \frac{I_1(a_1)}{I_0(a_1)}. \quad (7)$$

$I_1(a_1)$ and $I_0(a_1)$ are hyperbolic Bessel functions which are tabulated in many mathematical handbooks (as e.g. Abramowitz and Stegun [14]). A program (ratio of the Bessel functions) is available from one of the authors (H.G.).

If one is interested in the directed growth process in the three-dimensional space then the Eqns. (6) and (7) have to be replaced by

$$\begin{aligned} \langle \cos \Phi \rangle_{3\text{-dim}} &= 2\pi \int_{-\pi/2}^{+\pi/2} \cos \Phi \cdot f(\Phi) \cdot \sin \Phi \cdot d\Phi \\ &= \coth a_1 - \frac{1}{a_1}. \end{aligned} \quad (8)$$

The bidirectional growth process in a plane (focal plane of the microscope) can be quantified as the average of $\cos 2\Phi$

$$\langle \cos 2\Phi \rangle = \int_0^{2\pi} \cos 2\Phi \cdot f(\Phi) \cdot d\Phi. \quad (9)$$

$\langle \cos 2\Phi \rangle$ is +1, when all cells grow parallel or antiparallel to E . $\langle \cos 2\Phi \rangle$ is -1 when all the cells grow perpendicularly to E . $\langle \cos 2\Phi \rangle$ is zero when the cells grow randomly.

The bidirectional growth process in three-dimensional space can be quantified as the average of the second Legendre polynomial $P_2(\cos \Phi)$

$$\langle P_2 \rangle = 2\pi \int_{-\pi/2}^{+\pi/2} \frac{1}{2} (3\cos^2 \Phi - 1) \cdot f(\Phi) \cdot \sin \Phi \cdot d\Phi. \quad (10)$$

Results and Discussion

Directed growth

Short germ tubes of *N. crassa* growing in an electric field are nearly straight. This means that when a spore outgrows in a certain direction the germ tube maintains this direction for some time. The orientation of the germ tubes in an electric field can therefore be measured readily, and the average $\cos \Phi$, as a function of the applied electric field, can be determined. A plot of these measurements can be regarded as the dose-response curve. The electric field strength E which is applied to the cells is the dose and the cellular response is quantified by the average $\cos \Phi$ (Fig. 2a). The experimental data can be fitted to a theoretical curve (Eqn. (7)) if one knows the relationship between the coefficient a_1 and the applied electric field strength.

In weak electric fields a_1 is linear in E .

$$a_1(E) = K_{\text{GROW}} \cdot E. \quad (11)$$

The linear response of the cells to the applied electric field is described by K_{GROW} . The dose-response curve of short germ tubes is shown in Fig. 2a. All the measured values can be approximated to a linear function (Eqn. (11)) in connection with Eqn. (7).

The galvanotropic constant, K_{GROW} , describes how sensitive the spores are to the exogenous electric field. The best fit to the data of *N. crassa* provides a value of $K_{\text{GROW}} = (-20 \text{ V} \cdot \text{cm}^{-1})^{-1}$. The negative sign of K_{GROW} indicates that the germ

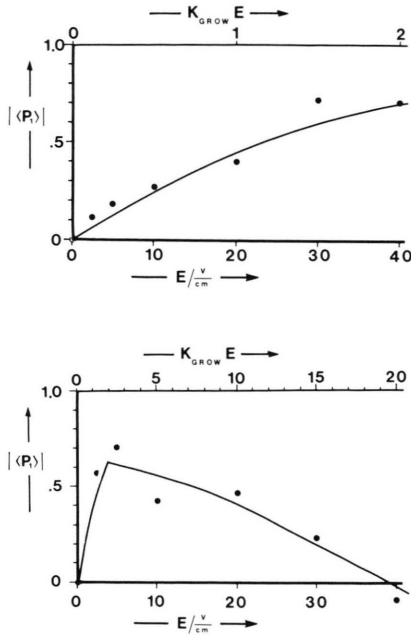


Fig. 2. Dose-response curve of a) spores ($K_{\text{GROW}}^{-1} = -20 \text{ V} \cdot \text{cm}^{-1}$, $l_0 = 10 \mu\text{m}$), b) parental hyphae ($K_{\text{GROW}}^{-1} = -2.3 \text{ V} \cdot \text{cm}^{-1}$, $K_1 = 1.106$, $l_0 = 100 \mu\text{m}$, and $E_0 = 3.8 \text{ V} \cdot \text{cm}^{-1}$). The data are taken from McGillivray and Gow [5]. The lines are theoretical predictions (Eqns. (7), (11), and (13)).

tubes grow in general towards the anode, in the opposite direction to the electric field vector. K_{GROW} is also a function of the germ tube length since K_{GROW} is $(-20 \text{ V} \cdot \text{cm}^{-1})^{-1}$ for $10 \mu\text{m}$ germ tubes and $(-1.7 \text{ V} \cdot \text{cm}^{-1})^{-1}$ for $100 \mu\text{m}$ germ tubes. To describe this effect another coefficient, K_p (P for polar), is introduced as

$$K_{\text{GROW}} = \frac{l_0}{K_p}, \quad (12)$$

where l_0 is the size of the cell. K_p has the dimension of volts and its absolute value is proportional to the voltage drop along the membrane induced by the applied electric field. This means the actual primary cellular signal is proportional to the applied electric field strength times a characteristic length of the cell. K_p is -18.5 mV for conidia of *N. crassa*.

It is worth while noting that the galvanotactic responses of granulocytes [15] is very similar in its description to the galvanotropism of fungal spores. These experiments can also be described by a linear term and the coefficient is defined in the same way as for galvanotropism (Eqn. (12)): The

galvanotactic constant is $(-2 \text{ V} \cdot \text{cm}^{-1})^{-1}$. A voltage of -2 mV is obtained by taking $10 \mu\text{m}$ as a typical cell length [15].

The galvanotropic response of germ tubes longer than $100 \mu\text{m}$ cannot be described by a linear response in E . The dose-response curve for long germ tubes is shown in Fig. 2b. At low electric field strengths the average of $\cos \Phi$ increases with increasing E and at high electric fields the average of $\cos \Phi$ decreases with increasing E . The average $\cos \Phi$ can be used to determine the a_1 value by using Eqn. (7). (They are identical with those shown in Fig. 3.) a_1 increases linearly with increasing field strength but above a threshold value, E_0 ($= 3.8 \text{ V} \cdot \text{cm}^{-1}$), a_1 then decreases with increasing field strength.

$$a_1 = \frac{l_0}{K_p} \cdot (E - K_1(E - E_0)) \quad \text{for } E > E_0. \quad (13)$$

The low field strength ($E < E_0 = 3.8 \text{ V} \cdot \text{cm}^{-1}$ or $l_0 \cdot E_0 = 38 \text{ mV}$) are approximated by Eqn. (13) yielding a coefficient, K_p of (-18.5 mV) . The inhibition coefficient, K_1 , describing the response above the threshold field, E_0 , is 1.11. Galvanotaxis of granulocytes and neural crest cells at high electric field strengths is also described by Eqn. (13).

The galvanotropic response of the directed growth changes sign at a critical field strength E_{00} ($= E_0 \cdot K_1 \cdot (K_1 - 1)^{-1}$). This critical field strength was observed in several experiments. It seems that the response of *N. crassa* changes sign at a field strength of about $40 \text{ V} \cdot \text{cm}^{-1}$ (see Fig. 3). For hyphal tips and germ tubes of *Phycomyces* this critical field was actually observed. They grow towards the anode below $5 \text{ V} \cdot \text{cm}^{-1}$ and toward the cathode above $5 \text{ V} \cdot \text{cm}^{-1}$ [11].

The linear response and the inhibition of anodotropic growth at high electrical field strengths indi-

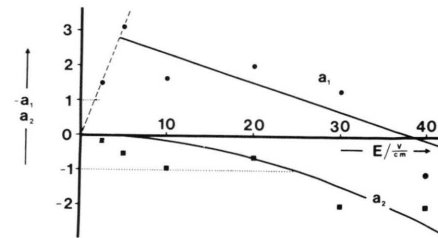


Fig. 3. Directed (a_1) and bidirectional (a_2) growth coefficient as a function of the applied electric field strength.

cates that the electric field can interact with the cell in two different ways. (i) The applied electric field may create an electric field parallel to the membrane surface so that charged membrane-bound proteins which are essential for galvanotropism are caused to migrate by lateral electrophoresis or electroosmosis. The distribution of the charged membrane-bound particles can be regarded as the primary cellular signal. The concentration difference of these particles at two parts of the membrane would then depend on the potential difference between these two points. This potential difference is proportional to the applied field strength and to the size of the cell and consequently one would expect that galvanotropism would be described by a coefficient which has the dimension of a voltage as actually found in this analysis. (ii) The applied electric field may also induce a change in the transmembrane potential difference. The disturbance would again be proportional to the applied field strength and to the size of the cell. The membrane potential difference and the ion concentrations inside and outside the cell act as a driving force for ion transport. If the membrane potential difference is altered when the ion concentrations in the cell are constant then there would exist a value where the flux of one type of ion can change its direction of movement. Substantial changes in the ion fluxes could occur when the membrane potential difference is altered by $l_0 \cdot E_0$ (inhibition) as well as $l_0 \cdot E_{00}$ (when the response to the field is changed in direction).

Bidirectional growth

The generating function can be obtained from the measured histograms which characterize the growth in an electric field. First the histograms for *N. crassa* were smoothed then the symmetry operation (Eqn. (3)) was applied in order to minimize the statistical error. In the last step the natural logarithm of the angle distribution function was plotted *versus* $\cos \Phi$. The results are shown in Fig. 4. All the histograms can be described using three coefficients $a_0(E)$, $a_1(E)$, and $a_2(E)$. The non-trivial parameters, $a_1(E)$ and $a_2(E)$, are shown in Fig. 3. $a_1(E)$ can be described by Eqns. (11), (12), and (13). The bidirectional growth described by a_2 can be approximated by

$$a_2(E) = K_2 \cdot (l_0 \cdot E)^n. \quad (14)$$

The exponent, n , describes the type of response. For example when $n = 1$, a direct interaction is obtained where the electric field can immediately interact with the cell. An induced interaction is obtained for $n = 2$ where the electric field induces a change in the cell and this cellular change establishes a new type of interaction with the electric field. The function of the exponent, n , is obvious in a physical system; for example with permanent and induced dipole interactions with electric fields. The direct interaction is due to the permanent electric dipole interaction with the applied field, yielding a linear dependency in E , and the induced interaction occurs when the electric field induces an electric dipole and this dipole interacts in turn with the applied electric field resulting in a E^2 dependence. Unfortunately the uncertainty in the data points is so large that we can not determine the exponent n . But below we will give some arguments which support an exponent of two. The bidirectional galvanotropic coefficient, K_2 , is $-(0.25 \text{ V})^{-2}$ for $l_0 = 100 \mu\text{m}$. The negative sign indicates that the bidirectional growth is perpendicular to the applied field. K_2 describes the natural sensitivity of the bidirectional state of the growing cells in an electric field. It is obvious that the directed and the bidirectional growing states of the parental hyphae have completely different sensitivities.

Transition from directional to bidirectional growth

One can predict the transition from the directional to bidirectional growth from the magnitude of the coefficients a_1 and a_2 . If $|a_1| > |a_2|$ the directed growth is more pronounced than the bidirectional one. However, if $|a_1| < |a_2|$ then the bidirectional growth is more pronounced than directed growth. The transition is postulated when $|a_1|$ equals $|a_2|$. From Eqns. (13) and (14) we obtain for $K_1 \sim 1$

$$l_0 \cdot E_T^2 = \frac{K_1 E_0}{K_2 K_p}, \quad (15)$$

where E_T is the electric field strength at the transition point. This result is obtained assuming that the bidirectional growth is an induced effect ($n = 2$). Eqn. (15) predicts that the transition is a function of the applied electric field strength as well as the size of the cells. If we use the values of the above determined coefficient ($K_p = -18.5 \text{ mV}$, $K_1 = 1.11$, $E_0 = 3.8 \text{ V} \cdot \text{cm}^{-1}$, and $K_2 = -(0.25 \text{ V})^{-2}$) we obtain for $l_0 \cdot E_T^2 = 14 \text{ V}^2 \cdot \text{cm}^{-1}$. McGillivray

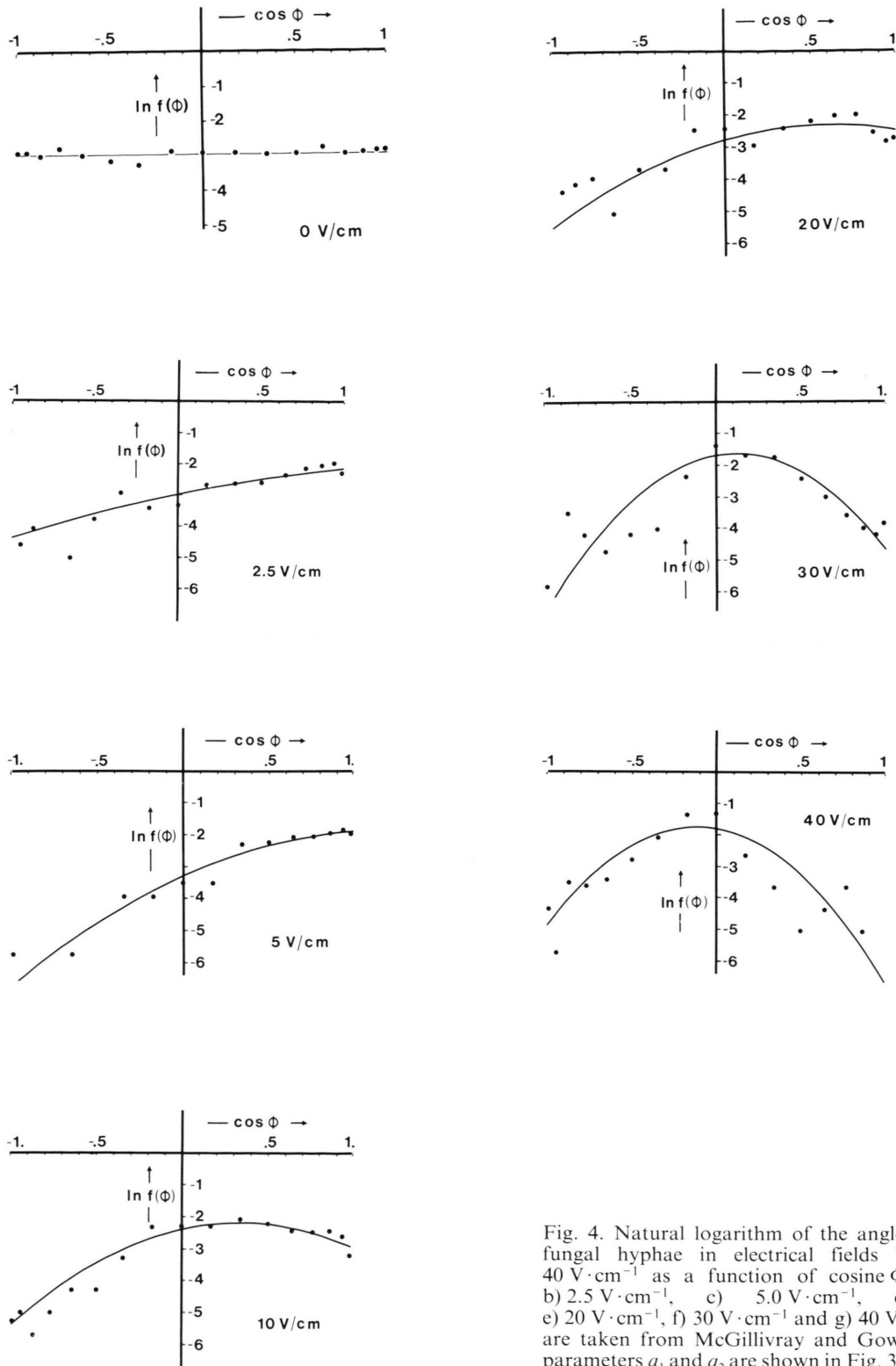


Fig. 4. Natural logarithm of the angle distribution of fungal hyphae in electrical fields between 0 and 40 $\text{V} \cdot \text{cm}^{-1}$ as a function of cosine Φ . a) 0 $\text{V} \cdot \text{cm}^{-1}$, b) 2.5 $\text{V} \cdot \text{cm}^{-1}$, c) 5.0 $\text{V} \cdot \text{cm}^{-1}$, d) 10 $\text{V} \cdot \text{cm}^{-1}$, e) 20 $\text{V} \cdot \text{cm}^{-1}$, f) 30 $\text{V} \cdot \text{cm}^{-1}$ and g) 40 $\text{V} \cdot \text{cm}^{-1}$. The data are taken from McGillivray and Gow [5]. The fitting parameters a_1 and a_2 are shown in Fig. 3.

and Gow [5] determined this transition from directional to bidirectional growth for different hyphal lengths. From their experiments one finds that the square of the transition field strength times the size of the cell describes the relation between the length at which the change in response occurred at different electrical field strengths as predicted by Eqn. (15). This suggests that the exponent, n , is two since the dimensions of the theoretical prediction and the experimental result are the same. The bidirectional growth of *N. crassa* is an induced effect. The experimentally determined value of $I_0 \cdot E_T^2$ is $4.4 \text{ V}^2 \cdot \text{cm}^{-1}$ (Fig. 5 of ref. [5]). The model does not predict very well the absolute value of $I_0 \cdot E_T^2$.

Bidirectional orientation is also observed in galvanotaxis of fibroblasts [1] and of neural crest cells [16]. The exponent, n , for the bidirectional orientation of fibroblast is two [1] and therefore the orientation is also an induced cellular response as in the bidirectional growth of *N. crassa*.

A possible model for the bidirectional orientation and growth can be proposed based on an accumulating inhibition of the directed migration or

growth as the electric field is increased. For simplicity let us assume the cells are spherical. The field-induced changes in the transmembrane potential difference is greatest at the membrane areas facing the anode and the cathode, and consequently we expect in these zones the greatest inhibition. There is no change in the transmembrane potential difference in those areas where the applied electric field is perpendicular to the normal of the membrane. We suggest that the strong electric fields may push the membrane areas with maximum sensitivity from the pole towards the equator. The electric field therefore act first in a direct way and then in an induced way on the cell. From this one predicts a response with a square dependence on the magnitude of the electric field.

Acknowledgement

One of us (H. G.) wants to thank the "Fonds der Chemischen Industrie" for supporting this work. N. A. R. G. thanks the SERC and AFRC for financial support.

- [1] C. A. Erickson and R. Nuccitelli, *J. Cell Biol.* **98**, 1708 (1983).
- [2] H. Gruler and R. Nuccitelli, *New Insights into Galvanotaxis and other Directed Cell Movements: An analysis of the translocation distribution function, in: Ionic Currents in Development* (R. Nuccitelli ed.), A. R. Liss Inc., New York 1986.
- [3] H. Gruler, *Biophysics of Leukocytes: Neutrophil Chemotaxis, Characteristics and Mechanisms*, in: *The Cellular Biochemistry and Physiology of Neutrophils* (M. B. Hallett, ed.), CRC Press UNISCIENCE (1989).
- [4] T. Matthes and H. Gruler, *Eur. Biophys. J.* **15**, 343 (1988).
- [5] A. M. McGillivray and N. A. R. Gow, *J. Gen. Microbiol.* **132**, 2515 (1986).
- [6] N. Patel and M. M. Po, *J. Neuroscience* **2**, 483 (1982).
- [7] F. W. Bentrup, *Z. Pflanzenphysiol.* **59**, 309 (1986).
- [8] O. Sand, *Exp. Cell Res.* **76**, 444 (1973).
- [9] E. J. Lund, *Bot. Gazette* **76**, 288 (1923).
- [10] T. H. Chen and L. F. Jaffe, *Planta* **144**, 401 (1979).
- [11] A. J. Van Laere, *FEMS Microbiol. Lett.* **49**, 111 (1988).
- [12] H. Haken, *Synergetics. Non-Equilibrium Phase Transitions and Self-Organization in Physics, Chemistry, and Biology*, Springer, Berlin, Heidelberg 1983.
- [13] H. Gruler, *Chemokinesis, Chemotaxis, and Galvanotaxis*, in: *Lecture Notes in Biomathematics* (W. Alt and G. Hoffmann, eds.), Springer, Berlin, Heidelberg 1990.
- [14] M. Abramowitz, I. A. Stegun, *Handbook of Math. Functions with Formulas, Graphs, and Math. Tables*, National Bureau of Standards Applied Mathematical Series 55, p. 355, 1964.
- [15] B. Rapp, A. de Boisfleury, and H. Gruler, *Eur. Biophys. J.* **16**, 313 (1988).
- [16] M. S. Cooper and R. E. Keller, *Proc. Nat. Acad. Sci. U.S.A.* **81**, 160 (1984).

